

Dust Particle Pair Correlation Functions and the Nonlinear Effect of Interaction Potentials

Jie Kong^{1b}, Ke Qiao, Lorin S. Matthews^{1b}, *Member, IEEE*, and Truell W. Hyde, *Member, IEEE*

Abstract—Dust kinetic temperature is a measure of the energy of the stochastic motion of a dust particle and is a result of the combination of the Brownian motion and the fluctuations in the dust charge and confining electric field. A method using the equilibrium value of the mean square displacement was recently introduced to obtain the dust kinetic temperature experimentally. As a follow up, this paper investigates the relationship between the dust kinetic energy derived from the mean square displacement technique and a technique using the probability distribution of the displacements obtained from random fluctuations of the dust particle. The experimental results indicate that the harmonic confinement potential acting on the dust particle can be obtained by combining the two methods, allowing the nonlinear effect of the confining force to be investigated. The thermal expansion in a 1-D vertical chain is discussed as a representative application as it is related to the nonlinear confinement force, or the asymmetric confinement potential.

Index Terms—Dusty plasmas, plasma diagnosis.

I. INTRODUCTION

THE kinetic energy of a dust particle in dusty plasma is a combination of Brownian motion and fluctuations of the electric field and dust charge [1]–[9]. Experimentally, the dust energy can be derived from the Gaussian velocity distribution, where the dust velocity is usually calculated from the position difference between subsequent frames of high-speed video of the particle motion. Recently, we introduced a dust kinetic energy measurement technique based on the mean square displacement (MSD) method [10]–[14]. Important information, such as the dust particle resonance frequency, neutral drag coefficient, and dust kinetic energy, can be easily extracted from the MSD experimental data. Since the MSD calculation uses only the displacement of the particles from the initial image frame, the cumulative errors inherent to other methods generated from the calculation of velocity can be reduced. Another benefit is that using the equilibrium value of the MSD to calculate the dust kinetic energy significantly reduces the influence of unwanted continuous coherent oscillations in the system confinement [10].

The position fluctuation of a single dust particle confined in a harmonic potential can be described by the Langevin

equation, for which 1-D motion [11] is given by

$$m\dot{v} = -m\gamma v - m\omega_0^2 x + R(t) \quad (1)$$

where m is the mass, γ is the Epstein friction coefficient [15], ω_0 is the resonance frequency, and $R(t)$ is a random force. The MSD solution to (1) is

$$\langle x^2 \rangle = A_0 \left[1 - \exp\left(-\frac{\gamma\tau}{2}\right) \left\{ \cos(\hat{\omega}\tau) - \frac{\gamma}{2\hat{\omega}} \sin(\hat{\omega}\tau) \right\} \right] \quad (2)$$

where $A_0 = (2E_k/m\omega_0^2)$ is the equilibrium value as $\tau \rightarrow \infty$ and $\hat{\omega} = (\omega_0^2 - (\gamma/2)^2)^{1/2}$. Experimental data for a particle's position fluctuation can be used to generate the MSD as a function of the elapsed time. A fit to this data using (2) then allows determination of the experimental parameters such as dust kinetic energy E_k (to prevent confusion with the material temperature of a dust particle, here E_k is used instead of the usually used $k_B T$), the Epstein drag coefficient γ , and the resonance frequency ω_0 . Since this technique is based solely on the fluctuating dust positions, it has the added benefit of requiring no external perturbation to the dusty plasma environment.

For a two-particle system, the correlated Langevin equations can be separated into two independent Langevin equations by using the center of mass (CM) coordinates and positions relative to the CM of the system. In this case, the equation of motion for the CM and relative coordinates exhibits a simple form similar to (1). In this case, the Langevin equation of motion for the relative coordinates also reflects the interaction between the two particles, which contributes to the overall confinement potential.

It is well known that approximating the confinement potential of an individual particle as a quadratic function of the displacement from equilibrium is generally adequate for small fluctuations or low dust kinetic energy. However, for higher dust kinetic energies, or a confinement potential having significant asymmetry, nonlinear effects can no longer be ignored. Additional terms of the form $B_2 x^2 + B_3 x^3 + \dots$, where B_i , $i = 2, 3, \dots$ are constants, must be added to (1) to model these forces more accurately. Obtaining a mathematical solution to the nonlinear equation that arises for a particle under forced oscillation is complicated [16], [17]. To obtain an analytical solution of the nonlinear Langevin equation with a random force term $R(t)$ [as shown in (1)] is much more difficult.

Experiments which allow one to obtain information about the nonlinear response of dust particles, especially the nonlinear interactions that can arise between dust particles, can yield deeper insight into the understanding of the dusty plasma properties. Asymmetric interaction forces acting on

Manuscript received September 27, 2018; revised February 8, 2019; accepted March 7, 2019. This work was supported in part by the NSF under Grant 1740203 and Grant 1414523 and in part by the National Aeronautics and Space Administration (NASA) Jet Propulsion Laboratory (JPL) Control under Grant 151701. The review of this paper was arranged by Senior Editor S. Portillo. (*Corresponding author: Jie Kong.*)

The authors are with the Center for Astrophysics, Space Physics, and Engineering Research, Baylor University, Waco, TX 76798-7310 USA (e-mail: j.kong@baylor.edu).

Color versions of one or more of the figures in this paper are available online at <http://ieeexplore.ieee.org>.

Digital Object Identifier 10.1109/TPS.2019.2906583

the dust particles, such as the ion drag force or the ion-focusing effect in the vertical direction [18], [19], are an area of increasing research interest [20].

In this paper, we present a technique for investigating the local confinement potential based on the distribution of dust particle position fluctuations and the MSD method. Section II provides the theoretical background for using the probability distribution function (pdf) of the particle positions to calculate the confining potential. Section III presents the results of applying these two methods to experimental data. A comparison of the position probability distribution and MSD techniques is presented in Section IV, and the feasibility of using these techniques to derive nonlinear coefficients of the interaction force is discussed. Section V presents an application of using the obtained nonlinear coefficient to study the 1-D thermal expansion coefficient. Conclusion is presented in Section VI.

II. THEORETICAL BACKGROUND

A two-particle correlation density distribution function $f(\vec{r}_1 - \vec{r}_2)$ represents a joint probability for the relative position between the two particles, with the corresponding pair correlation function defined as [21]

$$g_2(\vec{r}) = \langle f([r_{x1} - r_{x2}, r_{y1} - r_{y2}, z_1 - z_2]) \rangle. \quad (3)$$

For a two-particle system, the particle pair has cylindrical symmetry. Anticipating our experimental conditions, we take, $r_i = r_{xi}$, displacement from the horizontal direction (perpendicular to gravity) and $h_i = z_i$ to represent the position of each particle along the vertical direction (parallel to gravity). This allows (3) to be rewritten as

$$g_2(r, h) = \langle f([r_1 - r_2, h_1 - h_2], t) \rangle = \langle f([r, h], t) \rangle \quad (4)$$

where $r = r_1 - r_2$ and $h = h_1 - h_2$. Note that this form of (3) and (4) can also be used for the CM case (or sloshing mode) simply by making the replacement $r = (m_1 r_1 + m_2 r_2 / m_1 + m_2)$ and $h = (m_1 h_1 + m_2 h_2 / m_1 + m_2)$. Since the forces acting on the particle pairs are derived from potentials, the probability of finding a particle at any particular location is related to the potential energy distribution at that location. This can be described by Boltzmann's equation [22]–[28]

$$g_2(r, h) = a_0 \exp\left(-\frac{\varphi(r, h)}{E_k}\right) = a_0 \exp(-\psi(r, h)) \quad (5)$$

where a_0 is a constant, $\varphi(r, h)$ is the confining potential energy, and $\psi(r, h) = \varphi(r, h)/E_k$ is the dimensionless potential.

For small displacements about the equilibrium position $x = [r, h]$, $\varphi(x)$ can be expanded as

$$\begin{aligned} \varphi(x) &= \varphi_0 + \frac{\varphi'}{1!}(x - x_0) + \frac{\varphi''}{2!}(x - x_0)^2 + \frac{\varphi'''}{3!}(x - x_0)^3 + \dots \\ &= p_{\varphi 0} + p_{\varphi 1}(x - x_0) + p_{\varphi 2}(x - x_0)^2 + p_{\varphi 3}(x - x_0)^3 + \dots \end{aligned} \quad (6)$$

where primes denote the derivative with respect to x and $p_{\varphi i}$ represents the i th coefficient of the polynomials. A convenient potential zero can be chosen such that $p_{\varphi 0} = 0$ and $p_{\varphi 1} = 0$. Thus, for small displacements, the restoring force can

be linearized and the potential $\varphi(x) = p_{\varphi 2}x^2$ is quadratic in the displacement x , with coefficient $p_{\varphi 2} = (1/2)m\omega_0^2$, where ω_0 is the particle's resonance frequency. In the following, we will focus on the vertical direction h , i.e., $x = h$. Substituting (6) into (5) yields

$$\begin{aligned} \psi(h) &= \psi_0 - \ln(g_2(h)) \\ &= P_0 + P_1 \Delta h + P_2 \Delta h^2 + P_3 \Delta h^3 + \dots \end{aligned} \quad (7)$$

where $P_i = p_{\varphi i}/E_k$ and P_0 and P_1 are zero by the argument given above. Thus, for a linear restoring force, only P_2 contributes and

$$\psi(h) = \frac{\varphi(h)}{E_k} = P_2 \Delta h^2. \quad (8)$$

The coefficient P_2 may be determined experimentally by fitting the pdf of a particle's position with a Boltzmann distribution, as in (5). When the resonance frequency ω_0 is determined employing some other experimental method, for example, the MSD method, the particle temperature can then be derived using (8) and the experimentally determined coefficient P_2 .

As mentioned earlier, the dust kinetic energy E_k can also be derived by fitting the MSD calculated for a particle's fluctuating position with an equation of the form shown in (2) to determine the equilibrium value A_0 . The relationship between the value A_0 derived from the MSD and the coefficient P_2 derived from the pdf is given by

$$A_0 = \frac{1}{P_2} = \frac{2E_k}{m\omega_0^2} \quad (9)$$

which can then be employed to serve as a criterion for the validation of the experimental measurement of each value.

Combining the temperature derived from A_0 as obtained from the MSD method and the coefficient P_2 obtained from the pdf of the particle position, the confinement potential $\varphi(h)$ can then be obtained from (8).

This method may be extended to investigate the nonlinear effect of the dust particle confinement force by including the higher order terms shown in (7), which is now written as

$$\psi(h) = \frac{m\omega_0^2}{2E_k} \Delta h^2 + P_3 \Delta h^3 + P_4 \Delta h^4 + \dots \quad (10)$$

The coefficients of the higher order terms may be determined by fitting the dimensionless potential $\psi(h)$, calculated from the pair correlation function obtained from the experimental data (7) with a cubic or higher order equation.

III. EXPERIMENTAL APPLICATION

The experiment described here was performed in a modified gaseous electronics conference (GEC) radio frequency (RF) cell [29], filled with argon gas at a pressure of 13.3 Pa. An RF electrical field was produced by a pair of capacitively-coupled electrodes 8 cm in diameter, situated one above the other, and separated by a distance of 2.54 cm. The upper electrode was grounded, while the lower electrode was powered by an RF generator at a constant frequency of 13.56 MHz. The amplitude of the input RF signal ranged from 1.5 to 9.0 W. An open-ended glass box of dimension 10.5 mm \times 10.5 mm \times 12.5 mm (width \times depth \times height) with 2-mm wall thickness

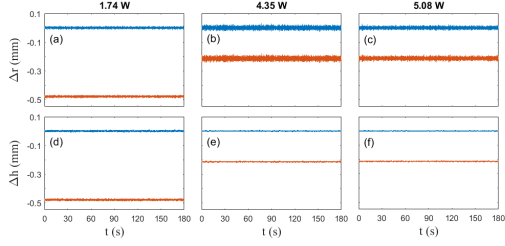


Fig. 1. Fluctuations in the (a)–(c) horizontal and (d)–(f) vertical directions for a two-particle vertical chain with RF power 1.74, 4.35, and 5.08 W, respectively. The separations between the upper and lower particles shown in the figure are all vertical distances (both particles are at the same mean horizontal positions under all the power settings). The mean vertical separations are 480, 215, and 213 μm for RF power 1.74, 4.35, and 5.08 W, respectively.

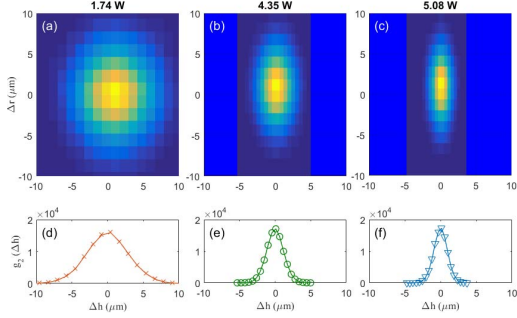


Fig. 2. Comparison of experimental results for the distribution function $f_2(r_1 - r_2, h_1 - h_2)$ collected at RF powers of (a) 1.74, (b) 4.35, and (c) 5.08 W, and the corresponding pair correlation function $g_2(\Delta h)$ at (d)–(f).

was placed at the center of the lower electrode. Melamine formaldehyde spheres having a manufacturer-specified mass density of 1.51 g/cm^3 and a diameter of $8.89 \mu\text{m}$ was used. A dust dropper was employed to introduce the particles into the glass box, where they were illuminated by a vertical sheet of laser light. The particles' positions were recorded at 500 frames per second (fps) using a side-mounted, high-speed CCD (photron) camera, and a microscope lens. Fig. 1 shows sample raw data of the fluctuations of the particle positions.

Because of the statistical nature of the correlation function, the sampling time for the experimental data must be long enough ($t_{\text{Sampling}} \rightarrow \infty$) to ensure the accuracy of the results. Accordingly, our experimental data were collected using a high-speed camera at 500 fps for a total duration of at least 3 min for each experimental run.

Employing the particle position fluctuation data shown in Fig. 1, the density distribution function and pair correlation function $g_2(h_1 - h_2)$ derived from data collected at 1.74, 4.35, and 5.08 W are shown in Fig. 2.

The dimensionless potential $\psi(\Delta h)$ is calculated from $g_2(\Delta h)$ using (7) with the resulting distribution fit employing a quadratic function as shown in (8). The results for various power settings are shown in Fig. 3.

The particle position data obtained from the experiment were also used to calculate the MSD as shown in Fig. 4 for various RF powers. The equilibrium value A_0 and the resonance frequency ω_0 were then derived from the theoretical fit obtained using (2).

As indicated in Fig. 4, the equilibrium value A_0 increases as the RF power decreases. It can also clearly be seen that

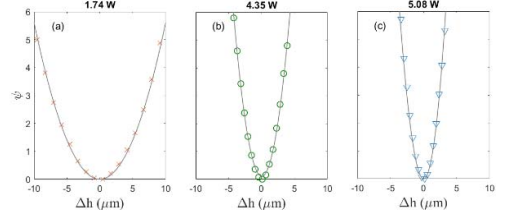


Fig. 3. (a)–(c) Experimental dimensionless interaction potentials $\psi(\Delta h)$ (symbols) at RF powers of 1.74, 4.35, and 5.08 W. Quadratic fits are indicated by solid lines. Each $\psi(\Delta h)$ is calculated from the corresponding g_2 shown in Fig. 2(d)–(f).

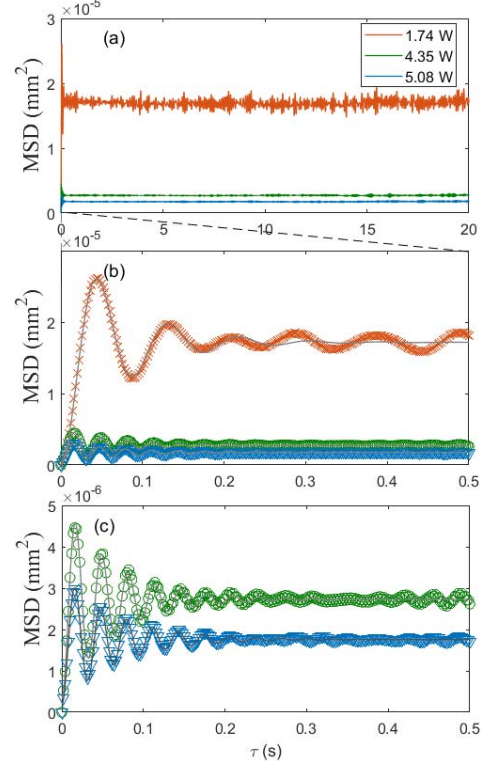


Fig. 4. (a) MSD's at RF power settings of 1.74, 4.35, and 5.08 W. (b) Corresponding expanded view of (a) for $\tau \leq 0.5\text{s}$ (symbols) and corresponding theoretical fits (solid lines) obtained using (2). (c) Details for 4.35 W and 5.08 W from (b).

the oscillation frequency increases as the RF power increases. These data are shown over a range of RF powers from 1.5 to 7.4 W in Fig. 5(a) and (b). The experimentally derived equilibrium value of the MSD, A_0 , and the inverse of the quadratic coefficient P_2 , obtained from the dimensionless potential ψ are compared in Fig. 5(a). As shown, the values are almost identical across the RF power range. Thus, the two methods yield consistent results, as required by the relationship given in (9).

The dust temperature can also be obtained from the MSD technique [see Fig. 5(c)], allowing the potential $\phi(h) = E_k \cdot \psi(h)$ to be calculated. In the following analysis, ϕ_2 and ϕ_3 are used to represent quadratic and cubic polynomials, respectively, for the potential fits.

IV. ANALYSIS AND DISCUSSION

As shown in Fig. 5(a), the experimental values for the equilibrium value A_0 of the MSD and the inverse of the quadratic parameter P_2 of the dimensionless potential ψ are

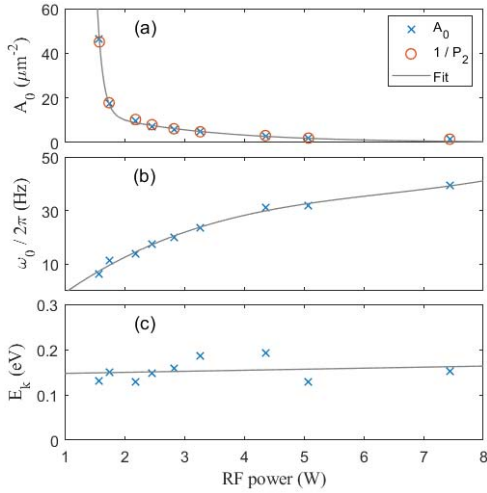


Fig. 5. (a) Comparison of A_0 and $1/P_2$ as a function of RF power. (b) Resonance frequency $\omega_0/2\pi$ derived from the MSD method illustrated in Fig. 4. (c) Dust kinetic energy calculated from $E_k = A_0 m \omega_0^2 / 2$ using the values from (a) and (b). The trend lines are shown to guide the eyes.

almost identical, as predicted by (9). It is important to note that the two techniques use entirely different statistical methods: the MSD technique is focused on the temporal correlations while the pdf method of using g_2 is determined by the fluctuations shown in the distribution of the spatial separations between the two particles. Thus, the experimental results shown in Fig. 5(a) confirm that the dust temperature derived from the MSD method represents the stochastic motions of the dust particle and are valid for use in the Boltzmann distribution (5) to determine the potential.

The advantages of using the MSD technique over other methods to derive the dust temperature are discussed in detail in [10]. In addition, the temporal distribution obtained from the MSD technique is self-sufficient, i.e., the dust temperature can be directly calculated from the measured values of A_0 and ω_0 , while the spatial (Boltzmann) distribution measured from the pdf of the particle positions must rely on other techniques to provide a separate measurement of the oscillation frequency ω_0 so that the dust kinetic energy E_k can be calculated from P_2 . However, there is one important advantage of using spatial distribution g_2 , the investigation of the nonlinearity of the interaction force.

As mentioned in Section I, to include nonlinear effects, the Langevin equation must be modified to include higher order terms

$$m\ddot{x} = -m\gamma\dot{x} - m\omega_0^2x + R(t) + B_2x^2 + B_3x^3 + \dots \quad (11)$$

It is difficult to solve (11) mathematically. In addition, for random fluctuations of small amplitude, it is questionable whether the deviations in the MSD result caused by any such nonlinear effects can be resolved experimentally. On the other hand, assuming a Boltzmann distribution representation for g_2 and fitting the dimensionless potential ψ employing a higher order polynomial, as expressed by (6) and (7), is simple, as shown in the example below.

In the following discussion, since the fluctuation amplitude is small, only the cubic term is included in the analysis. Therefore, the quadratic term remains the dominant term.

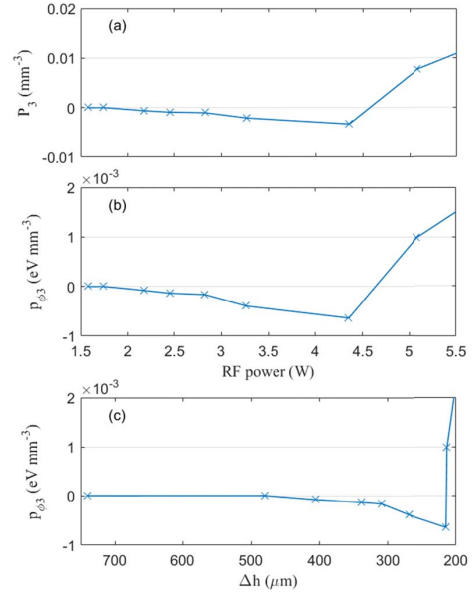


Fig. 6. (a) Cubic coefficient $p_{\phi 3}$ of the dimensionless potential ψ_3 as a function of the applied RF power. (b) $p_{\phi 3}$ of the confinement potential ϕ_3 as a function of the applied RF power. (c) $p_{\phi 3}$ as a function of the separation between the two particles.

The nonlinear coefficients P_3 and $p_{\phi 3}$ are derived from fitting the potential distributions $\psi(h)$ and $\phi(h)$, respectively. P_3 is derived by fitting the potential distribution $\psi(h)$ obtained from the spatial correlation g_2 , and $\phi(h) = E_k \cdot \psi(h)$, which also requires a value of the kinetic energy measured using the MSD method, is shown in Fig. 6(a) and (b) as a function of RF power. The potential is also shown as a function of the vertical particle separation in Fig. 6(c).

As can be seen in Fig. 6(c), for large separation, i.e., $h > 400 \mu\text{m}$, $p_{\phi 3}$ is close to zero, implying that the potential is parabolic. For separations between $214 < h < 400 \mu\text{m}$, $p_{\phi 3}$ is negatively increasing in magnitude as the separation decreases. It is important to note that rapid sign change from negative to positive occurs as the particle separation decreases to $h \sim 214 \mu\text{m}$. Since the cubic parameter $p_{\phi 3}$ represents the asymmetric shape of the confinement potential, its sign determines the “softer side” of the potential. The implications of this will be discussed in the following section.

V. ONE-DIMENSIONAL THERMAL EXPANSION COEFFICIENT

One of the applications of the nonlinear confinement force is to study the linear thermal expansion of a crystal structure. The linear thermal expansion of a 1-D crystal structure ΔL as a function of the temperature change ΔT is given by [30]

$$\Delta L = \alpha_L L_0 \Delta T \quad (12)$$

where α_L is the linear thermal expansion coefficient and L_0 is the original length of the crystal (to compare our case, the temperature change in (12) can be modified to be $\Delta T = E_k/k_B$). Fig. 8 shows the thermal expansion in a Lennard-Jones potential [31].

As shown in Fig. 7, a particle will be confined at the potential minimum located at L_0 when its temperature is

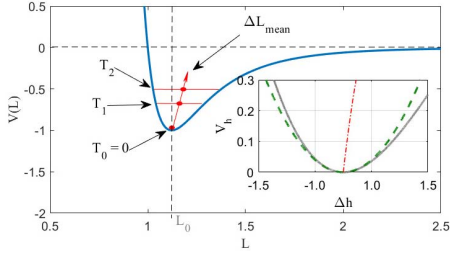


Fig. 7. Mean displacement ΔL_{mean} (relative to the zero-temperature equilibrium position L_0) in a Lennard-Jones potential, with the “softer side” of the potential for $L > L_0$, causes the mean displacement to increase as the confined particle temperature increases. Similarly, the inset shows a parabolic potential (dashed line) with a cubic function potential (solid line) with the nonzero mean displacement indicated (dashed-dotted line).

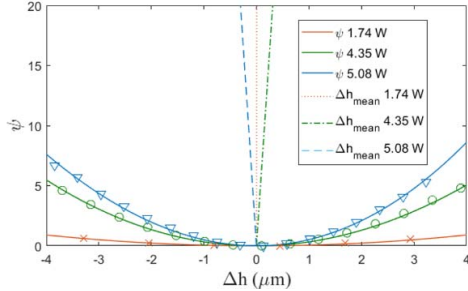


Fig. 8. Mean displacement relative to the equilibrium point at different particle energy levels (kinetic energy), calculated using the cubic potential obtained from experimental data (symbols). Solid lines are cubic fits to the potential for equilibrium separations of $480 \mu\text{m}$ (RF power 1.74 W), $215 \mu\text{m}$ (RF power 4.35 W), and $2.13 \mu\text{m}$ (RF power 5.08 W). The mean displacement at RF power 1.74 W , where the cubic coefficient is determined to be near zero, is almost expansion less.

$T_0 = 0$. As the particle temperature increases, the mean displacement will increase to $\bar{L} = L_0 + \Delta L_{\text{mean}}$, indicating a positive coefficient of thermal expansion. For small displacements (low particle temperature), the asymmetric potential can be described by a cubic polynomial. The sign of the cubic parameter determines the direction of the softer side. As shown in the inset, a cubic potential with a negative $p_{\phi 3}$ has a softer side for $\Delta h > 0$, as is seen in a Lennard-Jones potential. The softer side will move to $\Delta h < 0$ if the cubic parameter is positive. This will cause the mean displacement to decrease as temperature increases, which is the origin of negative thermal expansion [32]–[36]. Therefore, the cubic parameter $p_{\phi 3}$ can be used to study the linear thermal expansion. Cubic fits the experimentally measured potentials are shown in Fig. 8 for two different particle separations on either side of the critical value of $\Delta h = 214 \mu\text{m}$ shown in Fig. 6(c). At RF power 4.35 W , the particle separation is $215 \mu\text{m}$ and $p_{\phi 3}$ is negative, while the slightly smaller particle separation of $2.13 \mu\text{m}$ at 5.08 W yields a positive value of $p_{\phi 3}$.

As shown in Fig. 8, the mean displacement Δh_{mean} is zero for a parabolic potential ($p_{\phi 3} \sim 0$) at RF power 1.74 W (dotted line). As the RF power is increased to 4.35 W , the particle separation decreases to $215 \mu\text{m}$, and the cubic parameter changes to a negative value. The corresponding mean displacement Δh_{mean} increases positively as the particle energy level increases, indicative of a positive thermal expansion. As the RF power is further increased to 5.08 W , the cubic parameter $p_{\phi 3}$ changes to a positive value. The corresponding mean displacement Δh_{mean} increases negatively as the particle

energy level increases, which are a negative thermal expansion. This sign change is most likely related to the ion focusing effect [18], [19]. Changing the system RF power has an effect on the ion Mach number, moving the ion focusing region. It is speculated that the ion focusing region may change from a location between the two particles to a location which is downstream of both particles. But the exact cause for the sign change of $p_{\phi 3}$ is still unclear, needs further investigation, and other experimental techniques may be necessary, such as external heating.

VI. CONCLUSION

A comparison of experimentally determined kinetic energies and confinement potentials for an interacting pair of dust grains immersed in a complex plasma environment has been made using two different methods. The MSD method takes advantage of temporal correlations in the particles’ positions to determine the particles’ resonance frequency ω_0 from the evanescent oscillation (see Fig. 4).

On the other hand, the pdf takes advantage of the spatial variations in the particles’ positions. The experimental results shown in Fig. 5(a) confirm the theoretical equivalence of these two techniques. Therefore, either the MSD or pdf method can be used to examine the dust temperature, although the pdf method requires the resonance frequency to be measured separately using a different technique.

It is important to note that the use of the pdf method offers the advantage that the potential derived experimentally is the actual local confinement potential, making no *a priori* assumptions about its form. Given small fluctuation amplitudes, the simplifying assumption that the confining force is linear may be made, allowing the potential to be treated as quadratic. The nonlinear effects of the confinement force can be investigated by including the contribution of an additional cubic term in the potential. The result shows that at large separation distances the nonlinear coefficient is almost zero. As the separation distance decreases the nonlinear coefficient becomes negative. Interestingly, a transition occurred at $h \sim 214 \mu\text{m}$, where the nonlinear coefficient rapidly changes sign from negative to positive as the particle pair separation decreases. The asymmetric confinement potential is related to the structural linear thermal expansion when the cubic parameter of the confinement potential is not zero. When the sign of the cubic parameter of the asymmetric confinement potential is negative, the linear thermal expansion is normal, i.e., the structure dimension increases as the thermal kinetic energy increases. Our experimental result shows that a negative linear thermal expansion occurred as $h < 214 \mu\text{m}$. The exact cause for the sign change of $p_{\phi 3}$ is unclear and needs further investigation. It is possible that additional experimental techniques may be necessary, such as external heating. Both the MSD and the dust particle position pdf techniques described here are only suitable for confined dust particles.

REFERENCES

- [1] G. E. Morfill and H. Thomas, “Plasma crystal,” *J. Vac. Sci. Technol. A, Vac. Surf. Films*, vol. 14, no. 2, p. 490, 1996.
- [2] V. V. Zhakhovskii, V. I. Molotkov, A. P. Nefedov, V. M. Torchinski, A. G. Khrapak, and V. E. Fortov, “Anomalous heating of a system of dust particles in a gas-discharge plasma,” *J. Exp. Theor. Phys. Lett.*, vol. 66, no. 6, pp. 419–425, 1997.

- [3] R. A. Quinn and J. Goree, "Experimental investigation of particle heating in a strongly coupled dusty plasma," *Phys. Plasmas*, vol. 7, no. 10, pp. 3904–3911, 2000.
- [4] R. A. Quinn and J. Goree, "Single-particle Langevin model of particle temperature in dusty plasmas," *Phys. Rev.*, vol. 61, pp. 3033–3041, Mar. 2000.
- [5] O. S. Vaulina, S. A. Khrapak, A. P. Nefedov, and O. F. Petrov, "Charge-fluctuation-induced heating of dust particles in a plasma," *Phys. Rev.*, vol. 60, no. 5, pp. 5959–5964, 1999.
- [6] O. S. Vaulina, "Transport properties of nonideal systems with isotropic pair interactions between particles," *Plasma Phys. Rep.*, vol. 30, no. 8, pp. 652–661, 2004.
- [7] O. S. Vaulina, S. V. Vladimirov, A. Yu Repin, and J. Goree, "Effect of electrostatic plasma oscillations on the kinetic energy of a charged macroparticle," *Phys. Plasmas*, vol. 13, no. 1, 2006, Art. no. 012111.
- [8] U. Seifert, "Stochastic thermodynamics, fluctuation theorems and molecular machines," *Rep. Prog. Phys.*, vol. 75, no. 12, 2012, Art. no. 126001.
- [9] Y. Feng, J. Goree, and B. Liu, "Errors in particle tracking velocimetry with high-speed cameras," *Rev. Sci. Instrum.*, vol. 82, no. 5, 2011, Art. no. 053707.
- [10] J. Kong, K. Qiao, L. S. Matthews, and T. W. Hyde, "Temperature measurement of a dust particle in a RF plasma GEC reference cell," *J. Plasma Phys.*, vol. 82, no. 5, 2016, Art. no. 905820505.
- [11] P. Langevin, "On the theory of brownian motion," *Amer. J. Phys.*, vol. 65, no. 11, 1997.
- [12] R. Kubo, "The fluctuation-dissipation theorem," *Rep. Prog. Phys.*, vol. 29, pp. 255–284, Jan. 1968.
- [13] T. Li and M. G. Raizen, "Brownian motion at short time scales," *Ann. Physik*, vol. 525, no. 4, pp. 281–295, 2013.
- [14] T. Li, S. Kheifets, D. Medellin, and M. G. Raizen, "Measurement of the instantaneous velocity of a Brownian particle," *Science*, vol. 328, no. 5986, pp. 1673–1675, 2010.
- [15] P. S. Epstein, "On the resistance experienced by spheres in their motion through gases," *Phys. Rev.*, vol. 23, pp. 710–733, Jun. 1924.
- [16] H. G. Kadji, B. R. N. Nbandjo, J. B. C. Orou, and P. K. Talla, "Nonlinear dynamics of plasma oscillations modeled by an anharmonic oscillator," *Phys. Plasmas*, vol. 15, no. 3, 2008, Art. no. 032308.
- [17] A. F. El-Bassiouny and M. Eissa, "Dynamics of a single-degree-of-freedom structure with quadratic, cubic and quartic non-linearities to a harmonic resonance," *Appl. Math. Comput.*, vol. 139, no. 1, pp. 1–21, 2003.
- [18] M. Lampe *et al.*, "Trapped ion effect on shielding, current flow, and charging of a small object in a plasma," *Phys. Plasmas*, vol. 10, no. 5, pp. 1500–1513, 2003.
- [19] M. Lampe, V. Gavrishchaka, G. Ganguli, and G. Joyce, "Effect of trapped ions on shielding of a charged spherical object in a plasma," *Phys. Rev. Lett.*, vol. 86, no. 23, pp. 5278–5281, 2001.
- [20] W. J. Miloch, "Simulations of several finite-sized objects in plasma," *Procedia Comput. Sci.*, vol. 51, pp. 1282–1291, 2015. doi: [10.1016/j.procs.2015.05.313](https://doi.org/10.1016/j.procs.2015.05.313).
- [21] G. E. Astrakharchik, G. D. Chiara, G. Morigi, and J. Boronat, "Thermal and quantum fluctuations in chains of ultracold polar molecules," *J. Phys. B, At. Mol. Opt. Phys.*, vol. 42, no. 15, 2009, Art. no. 154026.
- [22] D. C. Prieve, "Measurement of colloidal forces with TIRM," *Adv. Colloid Interface Sci.*, vol. 82, Oct. 1999, Art. no. 93.
- [23] M. A. Brown, A. L. Smith, and E. J. Staples, "A method using total internal reflection microscopy and radiation pressure to study weak interaction forces of particles near surfaces," *Langmuir*, vol. 5, no. 6, pp. 1319–1324, 1989.
- [24] M. A. Brown and E. J. Staples, "Measurement of absolute particle-surface separation using total internal reflection microscopy and radiation pressure forces," *Langmuir*, vol. 6, no. 7, pp. 1260–1265, 1990.
- [25] V. Blickle, T. Speck, L. Helden, U. Seifert, and C. Bechinger, "Thermodynamics of a colloidal particle in a time-dependent nonharmonic potential," *Phys. Rev. Lett.*, vol. 96, Feb. 2006, Art. no. 070603.
- [26] N. A. Frej and D. C. Prieve, "Hindered diffusion of a single sphere very near a wall in a nonuniform force field," *J. Chem. Phys.*, vol. 98, no. 9, pp. 7552–7564, 1993.
- [27] M. A. Bevan and D. C. Prieve, "Hindered diffusion of colloidal particles very near to a wall: Revisited," *J. Chem. Phys.*, vol. 113, no. 3, pp. 1228–1236, 2000.
- [28] S. Chandrasekhar, "Stochastic problems in physics and astronomy," *Rev. Mod. Phys.*, vol. 15, no. 1, pp. 1–89, 1943.
- [29] J. Kong, T. W. Hyde, L. Matthews, K. Qiao, Z. Zhang, and A. Douglass, "One-dimensional vertical dust strings in a glass box," *Phys. Rev. E, Stat. Phys. Plasmas Fluids Relat. Interdiscip. Top.*, vol. 84, no. 1, 2011, Art. no. 016411.
- [30] P. A. Tipler and G. Mosca, *Physics for Scientists and Engineers*, vol. 1. New York, NY, USA: W. H. Freeman Company, 2007.
- [31] J. E. Jones, "On the determination of molecular fields.—II. From the equation of state of a gas," *Proc. Roy. Soc. London. A, Math. Phys. Eng. Sci.*, vol. 106, no. 738, pp. 463–477, 1924.
- [32] K. Röttger, A. Endriss, J. Ihringer, S. Doyle, and W. F. Kuhs, "Lattice constants and thermal expansion of H₂O and D₂O Ice Ih between 10 and 265 K," *Acta Crystallograph. B*, vol. 50, no. 6, pp. 644–648, 1994.
- [33] M. C. Rechtsman, F. H. Stillinger, and S. Torquato, "Negative thermal expansion in single-component systems with isotropic interactions," *J. Phys. Chem. A*, vol. 111, no. 49, pp. 12816–12821, 2007.
- [34] V. A. Kuzkin, "Negative thermal expansion in single-component systems with isotropic interactions," *J. Phys. Chem. A*, vol. 118, no. 41, pp. 9793–9794, 2014.
- [35] Z. Liu, Y. Wang, and S.-L. Shang, "Origin of negative thermal expansion phenomenon in solids," *Scripta Mater.*, vol. 65, no. 8, pp. 664–667, 2011.
- [36] Z. Liu, Y. Wang, and S. Shang, "thermal expansion anomaly regulated by entropy," *Sci. Rep.*, vol. 4, Nov. 2014, Art. no. 07043.



Jie Kong received the B.S. degree from Sichuan University, Sichuan, China, and the Ph.D. degree in physics from Baylor University, Waco, TX, USA.

He is currently with Baylor University, where he is an Associate Research Professor with the Center for Astrophysics, Space Physics, and Engineering Research (CASPER). His current research interests include structure analysis and stochastic process in complex (dusty) plasmas.



Ke Qiao received the B.S. degree in physics from Shandong University, Jinan, China, and the Ph.D. degree in theoretical physics from Baylor University, Waco, TX, USA.

He is currently with Baylor University, where he is an Associate Research Professor with the Center for Astrophysics, Space Physics, and Engineering Research (CASPER). His current research interests include structure analysis, waves and instabilities, and phase transitions in complex (dusty) plasmas.



Lorin S. Matthews (M'09) received the B.S. and Ph.D. degrees in physics from Baylor University, Waco, TX, USA, in 1994 and 1998, respectively.

She is currently an Associate Professor with the Physics Department, Baylor University, and an Associate Director of the Center for Astrophysics, Space Physics, and Engineering Research (CASPER). Previously, she was with Raytheon Aircraft Integration Systems, Waco, TX, USA, as the Lead Vibroacoustics Engineer on NASA's SOFIA (Stratospheric Observatory for Infrared Astronomy) Project.



Truell W. Hyde (M'01) received the B.S. degree in physics from Southern Nazarene University, Bethany, OK, USA, and the Ph.D. degree in physics from Baylor University, Waco, TX, USA.

He is currently with Baylor University, where he is the Director of the Center for Astrophysics, Space Physics, and Engineering Research (CASPER) and also a Professor of physics. His current research interests include astrophysics and space physics as well as complex plasma physics, specifically particle-particle interactions, dust acoustic waves and instabilities, linear and nonlinear phenomena, and structural phase transition in dusty plasmas.